REPORT DOCUMENTATION PAGE

Form Approved
OMB No. 0704-0188

1. REPORT DATE *(DD-MM-YYYY)*	2. REPORT TYPE	3. DATES COVERED *(From - To)*
06-06-2019	Final	04-29-2014 to 04-30-2018

4. TITLE AND SUBTITLE

Applications of the Single Scatter Subtraction (S3) Method for Rough Surface Scattering
Cross Polarization in Rough Surface Scattering

5a. CONTRACT NUMBER

5b. GRANT NUMBER
N00014-14-1-0559

5c. PROGRAM ELEMENT NUMBER

6. AUTHOR(S)

Gary S. Brown
Kevin Diomedi

5d. PROJECT NUMBER

5e. TASK NUMBER

5f. WORK UNIT NUMBER

7. PERFORMING ORGANIZATION NAME(S) AND ADDRESS(ES)

Virginia Polytechnic Institute and State University
Office of Sponsored Programs
North End Center, 300 Turner Street NW, Suite 4200
Blacksburg, VA 24061-0001

8. PERFORMING ORGANIZATION REPORT NUMBER

9. SPONSORING/MONITORING AGENCY NAME(S) AND ADDRESS(ES)

ONR REG Atlanta
100 Alabama Street SW Suite 4R15
Atlanta, GA 30303-3104

10. SPONSOR/MONITOR'S ACRONYM(S)
ONR

11. SPONSOR/MONITOR'S REPORT NUMBER(S)

12. DISTRIBUTION/AVAILABILITY STATEMENT

Unlimited Distribution

13. SUPPLEMENTARY NOTES

14. ABSTRACT

This report summarizes progress in developing more physics-based modeling for dealing with scattering from two-dimensional rough surfaces. The approach builds upon a method based on subtracting all the single scattering terms from the integral in the Magnetic Field Integral Equation. This subtraction led to the discovery of a surface curvature dependent term that is equivalent to the classic Luneburg-Kline correction to the geometric optics current on the rough surface. A further result illustrates the effects of considering scattering from a finite portion of the rough surface and discusses the implications of this result.

15. SUBJECT TERMS

Scattering, Rough Surfaces, Integral Equation, Surface Truncation, Luneburg-Kline Term, Single versus Multiple Scattering Isolation

16. SECURITY CLASSIFICATION OF:			17. LIMITATION OF ABSTRACT	18. NUMBER OF PAGES	19a. NAME OF RESPONSIBLE PERSON
a. REPORT	b. ABSTRACT	c. THIS PAGE			Dr. Gary S. Brown
U	U	U	Unlimited	12	19b. TELEPHONE NUMBER *(Include area code)* 540-231-4467

REPORT CATEGORY: Final Report

FOR: Office of Naval Research, Code 33
ATTN: Dr. Steve Russell

TITLE: Cross Polarization in Rough Surface Scattering

GRANT: N00014-1-0559

INVESTIGATORS: Prof. Gary S. Brown (PI) and Kevin Diomedi
ElectroMagnetic Interactions Laboratory
Bradley Department of Electrical and Computer Engineering
Virginia Polytechnic Institute & State University
Blacksburg, VA 24061

DATE: 30 April 2018

ABSTRACT

This report summarizes the progress made in developing a more physics-based method for dealing with scattering from two-dimensional rough surfaces. A new approach comprising the splitting of the current induced on a conducting surface into single and multiple scatter components is developed. A closed form augmentation of the Kirchhoff current is obtained for the single scatter part and an integral equation is derived for the multiple scatter current. The single scatter current is obtained by a simple fitting of extensive numerical computations for one-dimensional, sinusoidal surfaces which produce a heretofore unknown dependence upon the surface curvature. This term is essentially the same as the second term in a Luneburg-Kline series but it differs from previous results in that it is associated with the current vice the scattered field. Surface parameter ranges of validity for this result are established and the effects of truncating the extended surface are obtained and shown to be physically plausible. Finally, computations are presented that indicate that the simple curvature result can also be used for a sum of sinusoidal surfaces.

INTRODUCTION

Electromagnetic wave scattering from the ocean surface is highly important to the Navy for numerous reasons. In the last few years the understanding and predicting of such scattering has been greatly aided by numerical solutions of the complex interactions between rough surfaces and the incident radar waves. These numerical solutions have proven to be both accurate and robust in so far as the classes or surface roughness they can deal with. However, there is one very important problem that they have not been able to solve and that is depolarization in the scattering process. Depolarization or cross polarization is the process whereby the polarization of the electromagnetic field incident upon a rough surface is changed when scattered by the rough surface. This change in the incident wave's polarization state is important because it may yield information on certain characteristics of the scattering surface. The fundamental reason why this problem has not been numerically solved is that it is critically dependent upon the two-dimensionality (2-D) of the surface roughness and present numerical models are not readily extendable to 2-D roughness. That

is, the extension from 1-D roughness (a corduroy surface) to a 2-D surface (an ocean surface) requires too much computer power and memory to practically solve the scattering problem.

One approach to overcoming this limitation is to re-investigate classical solution technique(s) for the potential to yield insight into this problem. That is, it may not be possible to solve the most general rough surface scattering problem but the "solution" may yield insight and understanding which can be used to empirically build upon. In particular the current induced on the surface of a perfectly conducting body satisfies an integral equation of the second kind called the Magnetic Field Integral Equation (MFIE) and the classical "solution" of this equation is an infinite series of iterations starting with the source or Kirchhoff term in the MFIE. However, it is well known that this series does not always converge and mathematically this failure to converge is a result of the eigenvalues of the integral operator falling outside the unit circle. Unfortunately, there is no known physical reason for this failure so it is very hard to overcome. The research reported herein is an attempt to use the simple concept of single and multiple scattering to overcome this convergence problem and render the straightforward use of iteration a viable solution technique.

BASIS OF THE ANALYSIS

For a 1-D or corduroy, perfectly conducting, rough surface that is planar in the mean the current induced on the surface by an incident field satisfies the following second kind integral equation;

$$J(x) = J_o(x) + \int G_{TX}(x,x')J(x')dx' \tag{1}$$

Where $G_{TX}(x,x')$ is the kernel of the integral equation and *TX* denotes the polarization of the incident field; *X=M for TM or vertical and X=E for TE or horizontal.* The hypothesis that forms the foundation of this work is that *the single scattering part of the total current* $J(x)$ *is not just* $J_o(x)$ *or the Kirchhoff or source current but there is more that needs to be removed from the integral so that it cannot interfere with the convergence of an iterative solution of (1).* To obtain the single scattering part of the current in (1), we add and subtract $J(x)$ to the current in the integral giving;

$$J(x) = J_o(x) + \bar{G}_{TX}(x)J(x) + \int G_{TX}(x,x')[J(x') - J(x)]dx' \tag{2}$$

where $\bar{G}_{TX}(x)$ is the integral over x' of $G_{TX}(x,x')$. Then solving for $J(x)$ yields the following;

$$J(x) = J_o(x)/[1 - \bar{G}_{TX}(x)] + \int [\frac{G_{TX}(x,x')}{\{1-\bar{G}_{TX}(x)\}}][J(x') - J(x)]dx' \tag{3}$$

Now with $J(x) = J_{ss}(x) + J_{ms}(x)$ where $J_{ss}(x)$ is the single scattering part of the current and $J_{ms}(x)$ is the multiple scattering part, we see that

$$J_{ss}(x) = J_o(x)/[1 - \bar{G}_{TX}(x)] \tag{4}$$

and the integral equation for the multiple scattering part of the total current is as follows;

$$J_{ms} = J_{oo}(x) + \int \left\{ G'_{TX}(x,x') - \frac{\bar{G}_{TX}(x)}{1-\bar{G}_{TX}(x)} \delta(x'-x) \right\} J_{ms}(x')dx' \qquad (5)$$

where the quantities appearing (5) are defined as;

$$\bar{G}_{TX}(x) = \int_{-\infty}^{+\infty} G_{TX}(x,x')dx' \qquad G'_{TX}(x,x') = G_{TX}(x,x')/[1-\bar{G}_{TX}(x)] \qquad (6)$$

and

$$J_{oo}(x) = \int G'_{TX}(x,x')[J_{ss}(x') - J_{ss}(x)]dx' \qquad (7)$$

The kernels appearing above depend on the polarization (TE or TM) of the incident field as shown below;

$$G_{TE}(x) = 2\frac{\partial G(x,x')}{\partial n}\sqrt{1+\zeta_{x'}^2(x')} \qquad (8a)$$

$$\frac{\partial G(x,x')}{\partial n} = \frac{-k_o}{4j}\frac{[-\zeta_x(x)(x-x') + (\zeta(x)-\zeta(x')]}{\sqrt{1+\zeta_x^2(x)}\sqrt{(x-x')^2+(\zeta(x)-\zeta(x')^2}} \cdot H_1^{(2)}(k_o\sqrt{(x-x')^2+[\zeta(x)-\zeta(x')]^2}) \qquad (8b)$$

$$G_{TM}(x) = 2\frac{\partial G(x,x')}{\partial n'}\sqrt{1+\zeta_{x'}^2(x')} \qquad (8c)$$

$$\frac{\partial G(x,x')}{\partial n'} = \frac{k_o}{4j}\frac{[-\zeta_{x'}(x')(x-x') + (\zeta(x)-\zeta(x')]}{\sqrt{1+\zeta_{x'}^2(x')}\sqrt{(x-x')^2+(\zeta(x)-\zeta(x')^2}} \cdot H_1^{(2)}(k_o\sqrt{(x-x')^2+[\zeta(x)-\zeta(x')]^2}) \qquad (8d)$$

In these equations, $k_o = 2\pi/\lambda_o$ is the electromagnetic wavenumber and λ_o is the wavelength, $z = \zeta(x)$ is the surface height relative to the plane at $z = 0$, $\zeta_x(x)$ is the surface slope at the point x and $H_1^{(2)}(\cdot)$ is the Hankel function of the second kind and order one.

The single scatter current $J_{ss}(x)$ is defined as the part of the total current that depends only upon what is happening at the point x; the multiple scatter part $J_{ms}(x)$ is determined by all the other points on the surface. So, the single scatter current at x is determined by the incident field and the

surface behavior at x only while the multiple scatter part at x is determined by the incident field and surface behavior at potentially all other points on the surface. Note that this is exactly what the results in (4) and (5) above predict. The terminology "single scatter" and "multiple scatter" are also known as "local" and "nonlocal" splitting in mathematics.

Equations (4) and (5) are the governing relations for the single and multiple scatter parts of the total current, respectively. The concept of this research is that subtracting the single scatter current from the total current and leaving just the multiple scatter part will lead to a more convergent iterative solution of (5). Equation (4) clearly indicates that the Kirchhoff current $J_o(x)$ is not the complete single scattering current. The factor $[1 - \bar{G}_{TX}(x)]^{-1}$ is polarization dependent and must be determined numerically. Equation (5) for the multiple scatter part of the current is an integral equation that must be solved after the single scatter current is calculated. The integral equation solution method is to be iteration because of its simplicity. These calculations were the goals of this investigation.

NUMERICAL ANALYSIS

The calculation of $\bar{G}_{TX}(x)$, according to using (8) in the first part of (6), would appear to be a relatively simple task; unfortunately, this was not the case. In order to obtain a better understanding of the behavior of this integral, it was decided to use a simple sinusoidal surface of the form;

$$\zeta(x) = b\, cos(k_s x) \tag{9}$$

where $\zeta(x)$ denotes the height of the surface above a $z = \zeta(0) = 0$ reference plane, b is the peak amplitude of the surface and k_s is the wavenumber of the surface roughness ($= 2\pi/\lambda_s$ where λ_s is the surface wavelength). An inspection of (8) indicates an integrand that is both oscillatory and slowly decaying to zero as $|x'| \to \infty$. Additionally, although not so obvious, there is a singularity of the integral when $k_s = k_o$ due to the vanishing of the oscillatory part of the integrand and the resulting integrand behaving like $1/\sqrt{|x - x'|}$ whose integral is infinite for infinite limits. With these considerations in mind, the following approach was used.

(A) The infinite limits in (6) were replaced by $\pm 10^6 \lambda_o$ and $\bar{G}_{TX}(x)$ was calculated for a range of normalized surface amplitudes (b/λ_o) and wavelengths (λ_s). A simple, physically plausible, empirical result was obtained as a result of this study.

(B) In order to determine the effect of truncating the infinite limits to limits smaller than $\pm 10^6 \lambda_o$, both asymptotic analytical and numerical analyses were carried out to find just how the new limits affected the end result for a range of normalized surface amplitudes (b/λ_o) and wavelengths (λ_s).

(C) Calculations of $\bar{G}_{TX}(x)$ were carried out to determine if and when multispectral surfaces could be treated using the simplified result obtained in (A).

As will be shown in the next section of this report, accomplishing (A) through (C) comprised intensive computations along with matching the results with empirical mathematical forms that represent known and/or anticipated results. This process of matching numerical with analytical

results is a new innovation that is essential to validating the numerical results and providing simplified mathematical forms that reduce the computational load for more complex surfaces.

DISCUSSION OF RESULTS

The results of the calculations in part (A) above were quite illuminating. They were obtained by starting with a relatively small value of normalized surface height, b/λ_o, and a large normalized surface wavelength, λ_s/λ_o because these conditions are rather characteristic of single scattering conditions. The numerical output which was expected to require a large matrix of outputs versus inputs clearly suggested that the result was simply determined by the normalized surface curvature, $\zeta_{xx}(x)/k_o$. With of aid of some additional fitting, the following dependence on the surface curvature $\zeta_{xx}(x)$ was established

$$\bar{G}_{TX}(x) = \tau_{TX}[\tfrac{\zeta_{xx}(x)}{2k_o}] \tag{10}$$

$$J_{ss}(x) = J_o/[1 - \tau_{TX}\tfrac{\zeta_{xx}(x)}{2k_o}] \tag{10a}$$

where $\tau_{TE} = +j$ and $\tau_{TM} = -j$ denotes the polarization dependence. TE implies that the incident electric field is parallel to the ridges and dips in the corduroy surface while TM represents the case where it is the magnetic field that is parallel to these features. The limitations of this result were found to be approximately;

$$\lambda_s \geq 5\lambda_o \ (k_s \leq k_o/5) \quad \text{and} \quad b \leq 0.5\lambda_o \tag{10b}$$

The bound on the surface wavelength is a consequence of the infinite value of $\bar{G}_{TM}(x)$ and $\bar{G}_{TE}(x)$ which occur when the surface wavelength equals λ_o, where λ_o is the electromagnetic wavelength. Even though $\lambda_s = 5\lambda_o$ is relatively far from $\lambda_s = \lambda_o$, the differences between the numerical results and the curvature result in (10) is noticeable. It should be noted that there is a second infinite value occurrence for TE when $\lambda_s = \lambda_o/2$ and this comes from the slope dependent factor under the square root factor in (8a). The physical meaning of these infinite values is as yet undetermined. However, when taken at face value it seems that the single scatter-multiple scatter dichotomy simply fails for small ($O(\lambda_o)$) values of the surface wavelength because the situation is so multiple scatter dominated. One final point is that even though the bounds in (10a) appear restrictive, they translate into a peak slope of $0.2\pi = 0.63 \approx 36°$ which is relatively large.

The use of essentially infinite limits in computing $\bar{G}_{TX}(x)$ in part (A) above implies an infinite extent plane wave as the incident field; such an incidence field is not physically possible and a bounded field must be used. However, it would be very advantageous to retain the results in (10) because they are both physically appealing and mathematically simple in form. In order to do this, it is necessary to understand the effects of truncating the integral limits in the expressions for $\bar{G}_{TX}(x)$ such as was carried out in (B). In the first stages of this truncation study, it was hoped that the numerical calculations would be amenable to a simple empirical result such as in (10); however, this was found not to always be the case. To overcome this problem, it was necessary to develop an analytic asymptotic approach that would provide an accurate, closed-form result for the *truncated*

kernel integral, denoted as $\bar{\bar{G}}_{TX}(x)$ with the double over-bar denoting the truncation. It is desired to truncate the integral limits to $[-\alpha, +\alpha]$ and this integral can be written as follows;

$$\int_{-\alpha}^{+\alpha} G_{TX}(x,x')dx' = \int_{-\infty}^{+\infty} G_{TX}(x,x')dx' - \int_{-\infty}^{-\alpha} G_{TX}(x,x')dx' - \int_{\alpha}^{+\infty} G_{TX}(x,x')dx' \qquad (11)$$

The infinite limits integral is known from (10); it is $\bar{G}_{TX}(x)$. If α/λ_o is chosen sufficiently large and $|x| \ll \alpha$, the asymptotic forms for $G_{TX}(x,x')$ can be used because $|x'|$ is very large in both semi-infinite intervals. These asymptotic forms lead to the two integrals being integrable resulting in a closed form result. Of course the asymptotic form of $G_{TX}(x,x')$ is only approximate so the result will have some error in it; it should increase in accuracy as $[-\alpha, +\alpha] \to (-\infty, +\infty)$. In addition the accuracy of the truncated solution is much less important than having an estimate of the effects of the truncation on the current and the scattered field. For example, if a very narrow-beam antenna is illuminating a rough surface this would amount to truncating the integration range for calculating $\bar{\bar{G}}_{TX}(x)$ and, hence, the induced rough surface current and the resulting scattered field. The results derived here will enable an estimate of the effect of the illumination-produced truncation on all three quantities. The results of carrying out the operations in equation (11) are given below for TM polarization and then TE as follows;

TM (or Vertical) Polarization

$$\bar{\bar{G}}_{TM}(x) = -j\frac{\zeta_{xx}(x)}{2k_o} + \frac{bk_s(1+j)}{2}\frac{exp(-jk_o\alpha)}{\sqrt{4\pi k_o\alpha}}\left\{\left[\frac{\exp(-jk_ox)}{\sqrt{\left(1+\frac{x}{\alpha}\right)}} + \frac{\exp(jk_ox)}{\sqrt{\left(1-\frac{x}{\alpha}\right)}}\right]\left[\frac{\exp(-jk_s\alpha)}{(1+K_s)} - \frac{\exp(jk_s\alpha)}{(1-K_s)}\right]\right\} \qquad (11a)$$

$$\left(\frac{b}{\lambda_o} = 0.05, \frac{\lambda_s}{\lambda_o} \geq 2\right) \quad \left(\frac{b}{\lambda_o} = 0.1, \frac{\lambda_s}{\lambda_o} \geq 3\right) \quad \left(\frac{b}{\lambda_o} = 0.5, \lambda_s/\lambda_o \geq 5\right) \quad \left(\frac{b}{\lambda_o} = 1.0, \lambda_s/\lambda_o \geq 7\right)$$

TE (or Horizontal) Polarization

$$\bar{\bar{G}}_{TE}(x) = j\frac{\zeta_{xx}(x)}{2k_o} + \frac{(1-j)\zeta_x(x)\exp(-jk_o\alpha)}{\sqrt{4\pi k_o\alpha}\sqrt{(1+\zeta_x^2(x)}}\left\{\left[-\frac{\exp[-jk_ox]}{\sqrt{\left(1+\frac{x}{\alpha}\right)}} + \frac{\exp[jk_ox]}{\sqrt{\left(1-\frac{x}{\alpha}\right)}}\right]\left(1 + \frac{(bk_s)^2}{4}\left[1 - \frac{1}{2}\left[\frac{\exp(j2\alpha k_s)}{(1-2K_s)} + \frac{\exp(-j2\alpha k_s)}{(1+2K_s)}\right]\right]\right)\right\} \qquad (11b)$$

$$\left(\frac{b}{\lambda_o} \leq 0.1, \frac{\lambda_s}{\lambda_o} \geq 3\right) \qquad \left(\frac{b}{\lambda_o} = 0.5, \lambda_s/\lambda_o \geq 5\right) \qquad \left(\frac{b}{\lambda_o} = 1.0, \lambda_s/\lambda_o \geq 7\right)$$

where $K_s = \frac{\lambda_s}{\lambda_o} = k_o/k_s$. The range of validity considered in this study was restricted in (B) to what were considered reasonable values of b/λ_o and λ_s/λ_o. Note that in order to achieve smaller values of λ_s/λ_o, it was necessary to reduce b/λ_o below the values given in (10b). The specific

results for each polarization are shown above following the specific approximate analytic form. A plot of these bounds is shown below. The forms in (11a) and (11b) are valid above the curves and not valid beneath the curves. That is, for a given value of $\frac{b}{\lambda_o}$ only corresponding values of λ_s/λ_o above the curves produce an error-free result for $\bar{\bar{G}}_{TX}(x)$.

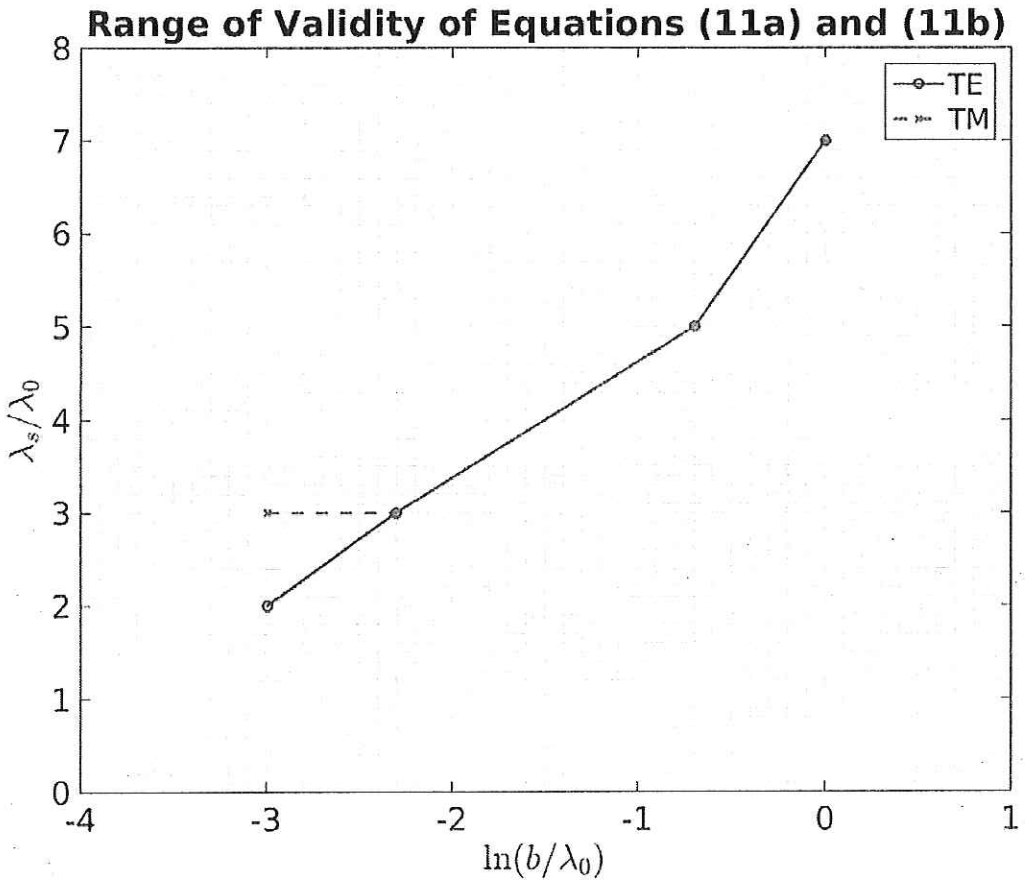

The only real difference between the parameter ranges for the two polarizations is that the TE results could be extended to $\frac{\lambda_s}{\lambda_o} \leq 3$. All of the calculations are valid for $\alpha/\lambda_o \geq 100$. It is very interesting to examine the electromagnetics contained in the α −dependent error terms in (11). First, they both go to zero when (a) $k_o\alpha \to \infty$ or (b) $bk_s \to 0$. The fact that the error term decays to zero as $[4\pi k_o\alpha]^{-1/2}$ is a distance dependent propagation consequence of the one dimensionality of the surface roughness. The first term inside the left curly bracket is a cylindrical standing wave caused by reflections from the truncation points at $x = \pm\alpha$. This term also predicts that $\bar{\bar{G}}_{TX}(x)$ will become very large when $x \to \pm\alpha$ because of the square root singularity there and indeed this has been observed in the numerically integrated values of $\bar{\bar{G}}_{TX}(x)$. The second square bracketed term inside the curly brackets is a consequence of the roughness slope that appears in (8a) and (8c) for the two polarizations. The TM result is simpler in form for it only has a linear slope term whereas TE contains an additional term $\sqrt{1+\zeta_{x'}^2(x')}$.

In regard to multispectral surfaces, the calculations referred to in (C) were numerous but not comprehensive. That is, they focused on the addition of surface wavelengths that were relatively close together because this was considered to be a good test of superposition. The calculations of $\bar{\bar{G}}_{TX}(x)$ were carried out using three different approaches. The baseline calculation entailed adding the individual surfaces together to generate a composite surface and then computing $\bar{\bar{G}}_{TX}(x)$. The second approach calculated $\bar{\bar{G}}_{TX}(x)$ for each surface wavelength and then added all the individual values of $\bar{\bar{G}}_{TX}(x)$ to generate a composite value of $\bar{\bar{G}}_{TX}(x)$. Finally, the empirical results for $\bar{\bar{G}}_{TX}(x)$ were calculated for each surface and then added together for the composite surface. This three-fold approach can probably be best explained by the following mathematical representations of the three computations.

First Approach:

$$\bar{\bar{G}}_{TX}(x)_1 = \bar{\bar{G}}_{TX}\big(x, \zeta_\Sigma(x)\big) \quad : \quad \zeta_\Sigma(x) = \textstyle\sum_{i=1}^{N} \zeta_i\,(x) \tag{12}$$

Second Approach:

$$\bar{\bar{G}}_{TX}(x)_2 = \textstyle\sum_{i=1}^{N} \bar{\bar{G}}^{i}_{TX}\,(x, \zeta_i(x)) \tag{13}$$

Third Approach:

$$\bar{\bar{G}}_{TX}(x)_3 = \textstyle\sum_{i=1}^{N} [\bar{\bar{G}}^{i}_{TX}(x, \zeta_i(x)]_e \tag{14}$$

In these expressions, $\zeta_i(x), i = 1 \ldots N$ are the N cosine surfaces corresponding to different wavelengths and amplitudes and the subscript "e" in the Third Approach denotes the empirical expression for $\bar{\bar{G}}^{i}_{TX}(x, \zeta_i(x))$. When using different values of peak surface height (b/λ_o), slope (bk_s), and curvature (bk_s^2) for each surface, it is necessary to use root-mean-square values as given below;

$$\frac{\zeta_{rms}}{\lambda_o} = \frac{1}{\sqrt{2}}\left\{\frac{1}{N}\textstyle\sum_{1=1}^{N}\left[\frac{b_i}{\lambda_o}\right]^2\right\}^{1/2} \qquad (\zeta_x)_{rms} = \frac{2\pi}{\sqrt{2}}\left\{\frac{1}{N}\textstyle\sum_{1=1}^{N}\left[\frac{b_i}{\lambda_o}\left(\frac{\lambda_o}{\lambda_s}\right)\right]^2\right\}^{1/2}$$

$$\lambda_o(\zeta_{xx})_{rms} = \frac{(2\pi)^2}{\sqrt{2}}\left\{\frac{1}{N}\textstyle\sum_{1=1}^{N}\left[\frac{b_i}{\lambda_o}\left(\frac{\lambda_o}{\lambda_s}\right)^2\right]^2\right\}^{1/2} \tag{15}$$

For the numerical results obtained in this study, all the surfaces were cosines and no phase shifts in the individual components were used. These simplifications were largely a result of the calculation of all three approaches above and certainly can and should be eliminated in the future.

For these calculations, all the amplitudes of individual surface components were taken equal and computations were carried out for two and some three surface wavelengths components. Emphasis was placed on composite surfaces with very closely spaced wavelengths because this gave a very large composite amplitude near $x = 0$ and was a good test of the various ways of supposing noted above. The purpose of the multi-wavelength computations was to determine the limits of the empiric results contained in (10) and (11). Computational results are shown in the table below.

λ_s/λ_0	$\zeta_{x_{rms}} \approx 0.30$	$\zeta_{x_{rms}} \approx 0.35$	$\zeta_{x_{rms}} \approx 0.40$	$\zeta_{x_{rms}} \approx 0.45$
{7,8}	$\zeta_{xx_{rms}}\lambda_0 \approx 0.25$	$\zeta_{xx_{rms}}\lambda_0 \approx 0.30$	$\zeta_{xx_{rms}}\lambda_0 \approx 0.34$	$\zeta_{xx_{rms}}\lambda_0 \approx 0.38$
{7,20}	$\zeta_{xx_{rms}}\lambda_0 \approx 0.26$	$\zeta_{xx_{rms}}\lambda_0 \approx 0.30$	$\zeta_{xx_{rms}}\lambda_0 \approx 0.34$	$\zeta_{xx_{rms}}\lambda_0 \approx 0.38$
{19,20}	$\zeta_{xx_{rms}}\lambda_0 \approx 0.097$	$\zeta_{xx_{rms}}\lambda_0 \approx 0.11$	$\zeta_{xx_{rms}}\lambda_0 \approx 0.13$	$\zeta_{xx_{rms}}\lambda_0 \approx 0.15$
{20,40}	$\zeta_{xx_{rms}}\lambda_0 \approx 0.087$	$\zeta_{xx_{rms}}\lambda_0 \approx 0.10$	$\zeta_{xx_{rms}}\lambda_0 \approx 0.12$	$\zeta_{xx_{rms}}\lambda_0 \approx 0.13$
{10,15,20}	$\zeta_{xx_{rms}}\lambda_0 \approx 0.16$	*	*	$\zeta_{xx_{rms}}\lambda_0 \approx 0.244$
{7,8,9}	$\zeta_{xx_{rms}}\lambda_0 \approx 0.25$	*	*	$\zeta_{xx_{rms}}\lambda_0 \approx 0.36$

*Note the 0.35 and 0.40 rms slope cases were not run for the three frequency surfaces.

TABLE 1. This table gives the surface curvatures for the given component surface wavelengths and rms slopes

The results for two frequency surfaces show that in general the real component has smaller errors than the imaginary and the error increases as the slope is increased. A bound on the surface slope of about $\zeta_{x_{rms}} \approx 0.40$ was found by examining different combinations of surface wavelengths with corresponding amplitudes to give rms slopes of $\{0.30, 0.35, 0.40, 0.45\}$. For $\frac{\lambda_s}{\lambda_o} = \{20,40\}$,The error is very small and may be acceptable even up to $\zeta_{x_{rms}} \approx 0.45$. At this point, TM has an error of twice the numerical magnitude and more importantly it has lost desired closed curvature form. The error in both the real and imaginary parts is greatest around $\frac{x}{\lambda_o} = 0$. This is a consequence of phase congruity and maximum surface slope and seems to be true for all surfaces for which the wavelengths of the composite surface falls within the $[-\alpha, +\alpha]$ support. TM appears to fare worse than TE but both look acceptable on all surfaces up to $\zeta_{x_{rms}} \approx 0.40$. Only on the TM surface with short periods such as $\frac{\lambda_s}{\lambda_o} = \{7,8\}$ does the $\zeta_{x_{rms}} \approx 0.45$ case really become questionable with significant errors of about half the magnitude and in the phase. While some of the surface component amplitudes here are much larger than previously investigated, the fact that they are mostly linear is encouraging that the empiric and analytic single frequency results could be valid in this region and applied to spectral surfaces.

The three frequency surfaces were not examined in enough detail to determine if they follow the same bound of $\zeta_{x_{rms}} \approx 0.40$ but show promising preliminary results. While the longer period surfaces comprising $\frac{\lambda_s}{\lambda_o} = \{10,15,20\}$ behave like the two frequency surfaces with good agreement

even up to $\zeta_{x_{rms}} \approx 0.45$, the $\frac{\lambda_s}{\lambda_o} = \{7,8,9\}$ surface shows significant errors for this rms slope, but had good agreement for $\zeta_{x_{rms}} \approx 0.35$. Examining the rms curvature shows that the latter surface is significantly rougher than the former, but not more than the two frequency surfaces which had acceptable agreement up to a slope of $\zeta_{x_{rms}} \approx 0.45$. These results were run with a relatively short integration supports of $\frac{\alpha}{\lambda_o} = 100$ and since the error seems to largely be in the real component, it may be absolved for larger integration support due to the $1/\sqrt{\alpha}$ decay.

Clearly this investigation of superposing sinusoidal surface components should be carried further so that the validity of the results in (10) and (11) can be validated for composite surfaces.

SUMMARY & FUTURE RESEARCH

The most important outcome of this investigation is given by the single scattering current result given in (10a). This result has a very important physical foundation for if $|\frac{\zeta_{xx}(x)}{2k_o}| \ll 1$, the single scatter current reduces to

$$J_{ss}(x) \approx J_o[1 + \tau_{TX} \frac{\zeta_{xx}(x)}{2k_o}] \qquad (16)$$

and the two terms inside the square brackets are the first two terms of a Luneburg-Kline asymptotic high frequency expansion for the surface current on a conducting surface, i.e.,

$$J_{ss}(x) \sim J_o(x) \sum_{n=0}^{\infty} a_n(x) k_o^{-n}$$

where $a_o(x) = 1$, $a_1(x) = \tau_{TX}\, \zeta_{xx}(x)/2$ and the remaining $a_n(x)$ were found to be zero for the range of validity of (10). It is limited to the single scattering current because of what has been shown in [5]. This result is new in that (a) it has never previously been determined for an extended rough surface, (b) it has never been shown that it is a part of the single scattering current and (c) it is an expansion for the current and not the scattered field. One finds a good bit of discussion of the Luneburg-Kline asymptotic series and the $1/k_o$ term in the literature [1, 2, 3, 4] but these references all deal with the scattered field rather than the current. The result in (16) actually augments these other findings and should render them more accurate. It is interesting to note that the second term in the Luneburg-Kline series is contained in the single scatter current as predicted in [5]. The closed form of this current, though obtained from numerical results, also carries its range of validity given in (10b). This is very helpful as it does not usually accompany a purely analytic approximation; the result is also expected to produce interesting insight regarding the statistical moments of the field scattered from a randomly rough surface when the surface height, slope and curvature are stochastic variables. These analyses along with the extension to 2-D rough surfaces are strongly suggested.

The analytical results predicting the effects of truncating the range of integration to a finite range in the integration of $G_{TX}(x)$ are both useful and unique for they provide a very good estimate of

both the magnitude of the error and its physical source resulting from the truncation. For example, if it is desired to be more .quantitative in regard to the errors introduced by truncation, the results in (11a) and (11b) are a very attractive alternative to a full-up numerical integration in $\bar{\bar{G}}_{TX}(x)$.

The multispectral addition of surfaces of differing wavelengths showed that the simple curvature result is frequently sufficient to predict an accurate single scatter current. There are limitations when the number of surfaces is greater than two but this is expected to be a result of the need to lower the root-mean-square amplitude of the composite surface. This part of the study requires further investigation as there is a need for applying this work to random surfaces which are formed.

Finally, the issue of finding the multiple scatter part of the current by solving the integral equation that it must satisfy was not considered due to a lack of time. This part of the total current must be determined if multiple scatter is to be accounted for.

REFERENCES

1. S. W. Lee, "Electromagnetic reflection from a conducting surface: geometrical optics solution," *IEEE Trans. Antennas & Propaga.*, vol. AP-23, pp. 184 – 191, 1975.
2. P. Y. Ufimtsev, "Uniform asymptotic theory of diffraction by a finite cylinder," *SIAM J. Appl. Math.*, vol. 37, pp. 459 – 466, 1979.
3. A. K. Dominek, L.Peters & W.D. Burnside, "An additional physical interpretation in the Luneburg-Kline expansion, *IEEE Trans, Antennas & Propaga.*, vol. AP-35, pp. 406 – 411, 1987.
4. H. Ansorge, "First-order corrections to reflection and transmission at a curved dielectric interface with emphasis on polarization properties," *Radio Science*, vol. 22, pp. 993 – 998, 1987.
5. G. S. Brown, "An inherent limitation of the Luneburg-Kline representation for the current on a conducting body," *IEEE Trans. Antennas & Propaga.*, vol. 38, pp. 1889 – 1892, 1990.